Since January 2020 Elsevier has created a COVID-19 resource centre with free information in English and Mandarin on the novel coronavirus COVID-19. The COVID-19 resource centre is hosted on Elsevier Connect, the company's public news and information website.

Biochemical and Biophysical Research Communications 558 (2021) 79–85

Contents lists available at ScienceDirect

Biochemical and Biophysical Research Communications

journal homepage: www.elsevier.com/locate/ybbrc

Production in *Escherichia coli* of recombinant COVID-19 spike protein fragments fused to CRM197

Maria Laura Bellone [d], Andrea Puglisi [a], Fabrizio Dal Piaz [b], Alejandro Hochkoeppler [a, c, *]

[a] Department of Pharmacy and Biotechnology, University of Bologna, Viale Risorgimento 4, 40136, Bologna, Italy
[b] Department of Medicine, University of Salerno, Via Giovanni Paolo II 132, 84084, Fisciano, SA, Italy
[c] CSGI, University of Firenze, Via della Lastruccia 3, 50019, Sesto Fiorentino, FI, Italy
[d] PhD Program in Drug Discovery and Development, Department of Pharmacy, University of Salerno, Via Giovanni Paolo II 132, 84084, Fisciano, SA, Italy

ARTICLE INFO

Article history:
Received 11 April 2021
Accepted 15 April 2021
Available online 20 April 2021

Keywords:
COVID-19
Spike protein
CRM197
Protein chimera
Escherichia coli

ABSTRACT

During 2020, the COVID-19 pandemic affected almost 10^8 individuals. Quite a number of vaccines against COVID-19 were therefore developed, and a few recently received authorization for emergency use. Overall, these vaccines target specific viral proteins by antibodies whose synthesis is directly elicited or indirectly triggered by nucleic acids coding for the desired targets. Among these targets, the receptor binding domain (RBD) of COVID-19 spike protein (SP) does frequently occur in the repertoire of candidate vaccines. However, the immunogenicity of RBD *per se* is limited by its low molecular mass, and by a structural rearrangement of full-length SP accompanied by the detachment of RBD. Here we show that the RBD of COVID-19 SP can be conveniently produced in *Escherichia coli* when fused to a fragment of CRM197, a variant of diphtheria toxin currently used for a number of conjugated vaccines. In particular, we show that the CRM197-RBD chimera solubilized from inclusion bodies can be refolded and purified to a state featuring the 5 native disulphide bonds of the parental proteins, the competence in binding angiotensin-converting enzyme 2, and a satisfactory stability at room temperature. Accordingly, our observations provide compulsory information for the development of a candidate vaccine directed against COVID-19.

1. Introduction

CRM197 (Cross-Reacting-Material 197) is a variant of diphtheria toxin featuring a single site-specific substitution (G52E) which does not affect the deoxyribonuclease activity [1] but suppresses the ADP-ribosylating activity and the toxicity of the parental protein [2,3]. Remarkably, the immunogenicity of formaldehyde-treated CRM197 does not significantly differ from that of diphtheria toxoid [4]. Therefore, the chemical conjugation to CRM197 represents an ideal tool for the enhancement of the immunogenicity of low molecular mass antigens, a strategy currently used to produce several vaccines [5]. Accordingly, the poor immunogenicity of COVID-19 spike protein RBD [6] could be improved by its conjugation to CRM197. However, a more efficient approach to conjugation could be the construction of a fusion protein containing CRM197, or a fragment of it, and the RBD of SP. Considering the attention that fusion vaccines are gaining [7], we thought it of interest to attempt the construction of a protein chimera designed to increase the immunogenicity of COVID-19 spike protein RBD. This attempt was supported by our previous observation that CRM197 can be overexpressed at high levels in *Escherichia coli* [8]. Moreover, we reported that overexpressed CRM197 can be recovered from inclusion bodies under denaturing conditions, with subsequent refolding and purification steps conveniently leading to the isolation of homogeneous and catalytically active CRM197 [8,9]. Remarkably, it was recently shown that recombinant CRM197 features a tertiary structure which is essentially identical to that of the corresponding native protein produced by *Corynebacterium diphteriae* [10]. In addition, it was demonstrated that the immunogenicity of recombinant CRM197 does not significantly differ from the immunogenic response triggered by the native protein [10].

* Corresponding author. Department of Pharmacy and Biotechnology, University of Bologna, Viale Risorgimento 4, 40136, Bologna, Italy.
E-mail address: a.hochkoeppler@unibo.it (A. Hochkoeppler).

https://doi.org/10.1016/j.bbrc.2021.04.056
0006-291X/

2. Materials and methods

2.1. Protein overexpression

A synthetic gene coding for the protein chimera CRM197-RBD was obtained by Genscript (Piscataway, NJ, USA) and was cloned into the pET9a expression vector, using the *Nde*I and *Bam*HI restriction sites, generating the pET9a-CRM197RBD construct. Electrocompetent *E. coli* BL21(DE3) cells were then transformed with the pET9a-CRM197RBD construct, and transformants were selected on Petri dishes containing LB-agar medium supplemented with 40 μg/mL of kanamycin. Single colonies of purified transformants were used to inoculate 2 mL of LB-kanamycin medium, and the cells suspension was incubated at 37 °C for 15 h under constant shaking (180 rpm). The pre-cultures accordingly obtained were diluted (1:500) in fresh LB-kanamycin medium and grown at 30 °C for 9 h. Finally, overexpression of CRM197-RBD was induced with 1 mM IPTG for 15 h, at 15, 30, or 37 °C. At the end of induction cells were harvested by centrifugation (4,000 g, 30 min, 4 °C), and the cells pellets were stored at −20 °C until used.

An identical procedure was used to overexpress and analyze the presence of the CRM197-PEP protein chimera in *E. coli* BL21(DE3).

2.2. Protein purification

Cells pellets were resuspended in 50 mM Tris-HCl, 50 mM NaCl, 5 mM EDTA, 10 mM DTT (pH 8.5), homogenized with a cold glass potter, and subjected to sonication. The protein extract accordingly obtained was centrifuged (14,000 g, 20 min, 4 °C), the supernatant was discarded, and the pellet was resuspended in buffer A (50 mM Tris-HCl, 50 mM NaCl, pH 8.5) supplemented with 1% (v/v) Triton X-100. The suspension was mildly shaken for 10 min at room temperature, centrifuged and the pellet was resuspended and washed again in buffer A containing Triton X-100. Finally, the washed pellet containing the inclusion bodies (generated by induction of CRM197-RBD) was resuspended in buffer A containing 10 mM DTT and 6 M urea, and the suspension was incubated at room temperature for 12 h under mild shaking. At the end of this time interval, the sample was centrifuged (14,000 g, 20 min, 4 °C), and the supernatant was loaded (flow rate 0.5 mL/min) onto a HiTrap Q-HR 5 mL column (Cytiva, Marlborough, MA, USA), previously equilibrated with the buffer used to solubilize inclusion bodies. The column flow-through was dialyzed against buffer B (50 mM Tris-HCl, 50 mM NaCl, 3 mM cysteine, 0.3 mM cysteine, pH 8.0) containing 1 M urea. The dialyzed sample was finally loaded at 0.5 mL/min onto a HiTrap Heparin 5 mL column (Cytiva) equilibrated with the buffer used for dialysis. Once loaded the sample, the column was washed with 10 mL of equilibration buffer, and a reverse urea gradient (1–0 M) was applied (10 column volumes, 0.5 mL/min). At the end of the gradient, the column was washed with 10 mL of buffer B, and proteins were subsequently eluted with a NaCl gradient (0.05–1 M, 10 column volumes, 1 mL/min). Fractions of 0.9 mL were collected, and analyzed by SDS-PAGE. The best fractions according to the electrophoretic analysis were pooled and their protein concentration was determined according to Bradford [11].

2.3. Activity assays

The DNase activity of recombinant full-length CRM197 and CRM197-RBD was assayed according to Kunitz [12], using calf thymus DNA as substrate. To verify the quality of the DNA substrate, the activity of a standardized solution of DNase I from bovine pancreas was assayed. To this aim, the increase in Absorbance at 260 nm of a solution containing 100 mM acetate buffer (pH 5.0), 5 mM $MgCl_2$, 40 μg/mL of DNA, and enzyme was determined with a Cary Bio 300 spectrophotometer. The activity of recombinant full-length CRM197 or CRM197-RBD was assayed in the presence of 50 mM Tris-HCl (pH 7.6), 2.5 mM $MgCl_2$, 2.5 mM $CaCl_2$, 40 μg/mL of DNA, and enzyme. One Kunitz Unit was defined as the amount of enzyme producing an increase in Absorbance of 0.001 per minute.

2.4. Mass spectrometry

To verify the identity of proteins, spots were excised from gels and underwent trypsin in-gel digestion as previously reported [13]. The resulting peptides were analyzed by LC-MS/MS using a Q-Exactive instrument (Thermo-Fisher Scientific, Waltham, MA, USA) equipped with a nano-ESI source coupled with a nano-Ultimate capillary UHPLC (Thermo-Fisher Scientific) as reported elsewhere [14].

To identify the disulphide-bond pattern of the CRM197-RBD chimera, trypsin digestion was performed in solution incubating 30 μg of not-reduced protein with 50 ng of trypsin at 37 °C overnight. The peptides accordingly obtained were reduced with 25 mM DTT at 40 °C overnight. The mixture was acidified to a final concentration of 0.5% formic acid and analyzed by LC/MS/MS.

2.5. Dynamic light scattering

Dynamic light scattering experiments were performed with a Malvern Panalytical (Malvern, UK) Zetasizer Nano ZS system. All the measurements were recorded at 25 °C. Scattering was evaluated at an angle of 173°. Raw data were analyzed with the Zetasizer software (Malvern Panalytical), and the main peaks accordingly identified were further inspected using the Fityk program [15]. By this means, each peak was deconvoluted into a set of Gaussian distributions, and each component was interpreted as a homogeneous sub-population of the enzyme ensemble.

2.6. Circular dichroism

CD spectra were recorded over the 200–250 nm wavelength interval at a scan rate equal to 50 nm/min, using a Jasco J-810 spectropolarimeter. Protein samples were in PBS buffer, and the bandwidth was set at 1 nm. Sixteen scans per sample were acquired and averaged.

2.7. Surface plasmon resonance

The binding of CRM197-RBD to angiotensin-converting enzyme 2 (ACE2) was analyzed using a Biacore 3000 instrument (Cytiva) according to published procedures [16]. ACE2 surfaces were prepared on research grade CM5 sensor chips (Cytiva) by immobilizing the protein (50 μg/mL in 40 mM CH_3COONa, pH 5.0) using a standard amine−coupling protocol; this procedure led to an observed density of 30 kRU. CRM197-RBD was equilibrated and diluted in 0.1 M HEPES, 1.5 M NaCl, 0.03 M EDTA, 0.5% v/v surfactant P20 (pH 7.4), to obtain samples at five different concentrations (1, 2, 4, 8, and 32 nM, respectively).

Binding experiments were performed at 25 °C with 120 s of association time and 300 s of dissociation time (flow rate 30 μL/min). The observed curves were fitted to a single-site interaction model, yielding a single K_D. Sensorgrams elaboration was performed using the BIAevaluation software, provided by Cytiva.

3. Results and discussion

To graft the RBD of COVID-19 spike protein onto CRM197, we designed a synthetic gene, optimized for *E. coli* codon usage, coding

for the first 388 residues of the diphtheria toxin variant, and for amino acids 319–541 of spike protein (Supplementary Fig. S1A). In particular, the resulting CRM197-RBD chimera was conceived to replace the receptor domain of CRM197 (Fig. 1A) with the RBD of spike protein (Fig. 1B and 1C). It is important to note that the extended linker connecting the catalytic-transmembrane and the receptor domain of CRM197 was conserved in the chimera to facilitate the folding of SP RBD (Fig.s 1D-1F). In addition, a few mutations were introduced in CRM197-RBD: i) A379G, Y380S, and V390G were inserted to increase the rotational freedom of the protein region linking CRM197 to RBD; ii) C608S was used to avoid the engagement of C608 in un-correct disulphide bridges (Supplementary Fig. S1B).

The overexpression of CRM197-RBD in *E. coli* BL21(DE3) was tested by culturing at 30 °C the transformed host strain, and subsequently inducing for 15 h with 1 mM isopropyl β-D-1-thiogalactopyranoside (IPTG) the overexpression of the target protein at 15, 30, or 37 °C. Surprisingly, we did not detect CRM197-RBD in total protein extracts obtained from cultures induced at 15 °C (Fig. 1G). However, when induction was performed at 30 or 37 °C the overexpression of CRM197-RBD was detected (Fig. 1G) and confirmed by mass-spectrometry (Supplementary Fig. S2). Moreover, the yield of target protein was high under both these conditions, being located in inclusion bodies (Fig. 1H). Accordingly, CRM197-RBD was solubilized with 6 M urea from inclusion bodies of cells induced at 37 °C, and we used anion-exchange chromatography as a first purification step. This was important to discard the portion of CRM197-RBD associated to nucleic acids (Supplementary Fig. S3). In particular, by UV spectroscopy we observed that the proteins retained by the column were heavily contaminated with nucleic acids while the column flow-through featured an absorption spectrum suggesting the presence of low amounts, if at all, of DNA and/or RNA. Accordingly, to pursue CRM197-RBD purification the flow-through from the anion-exchange column was subjected to dialysis, lowering the concentration of urea to 1 M, and the dialyzed protein pool was finally purified using a HiTrap Heparin column (Fig. 2A and 2B). It is interesting to note that a small fraction of purified CRM197-RBD was cleaved during overexpression, as revealed by reducing SDS-PAGE (Fig. 2B) and by mass spectrometry (Supplementary Fig. S4). Nevertheless, the far-UV CD spectrum of purified CRM197-RBD is diagnostic of a correct folding (Fig. 2C). Moreover, a comparison with the CD spectrum of full-length recombinant CRM197 (overexpressed in *Pseudomonas fluorescens*) did not disclose major differences between the two proteins (Fig. 2C). Further, when analyzed by dynamic light scattering (DLS), CRM197-RBD was detected as a single peak (Fig. 2D), albeit featuring a positive skew (Fig. 2E). Remarkably, it is important to note the absence of any major aggregates of very large diameter, i.e. $\geq$ 100 nm (Fig. 2D). The maximum of the CRM197-RBD peak corresponds to an apparent diameter equal to 24.6 nm. However, deconvolution by means of Gaussian functions suggests the presence of 6 components yielding the observed skewed peak (Supplementary Fig. S5A). In particular, the diameters of these components were estimated equal to 14.3,17.2, 21.4, 27.5, 36.4, and 48.6 nm, respectively (Supplementary Figs. S5A-S5B). When full-length recombinant CRM197 was subjected to DLS analysis, a complex pattern was observed, revealing the presence of the monomeric protein and two additional peaks diagnostic of aggregates featuring small- and large-diameter (Fig. 2F). When 3 independent DLS analytic runs of recombinant CRM197 were averaged, we estimated diameters equal to 6.07 ± 0.33, 15.5 ± 0.7, and 95.5 ± 2.6 nm, respectively (Supplementary Figs. S5C-S5D). CRM197 is known to associate into homodimers by the swapping of the receptor binding domains of two monomers [17]. This was also observed with recombinant CRM197 [10], and an inspection of the tertiary structure of this dimeric form reveals a diameter of approximately 10 nm (PDB file 5i82, Supplementary Fig. S5E). Therefore, the oligomer detected both in CRM197-RBD and in recombinant CRM197, and respectively featuring a diameter equal to 14.3 and 15.5 nm, cannot be interpreted as a dimer. We propose that this aggregated form is induced by RBD swapping with the generation of a linear or cyclic tetramer, as it was reported for diphteria toxin oligomers [18]. The CRM197-RBD chimera does contain 10 cysteines, of which 2 and 8 arise from CRM197 and from the RBD of COVID-19 SP, respectively. The 5 disulphide bonds in which these cysteines are engaged are reported in Supplementary Table 1, showing the coordinates relative both to the progenitor proteins and to the CRM197-RBD chimera. When the reconstitution of the correct disulphide bonds in the refolded chimera was tested by mass spectrometry, we unambiguously detected the presence of all the native S–S bridges (Fig. 3). This correct pairing between cysteines couples was most likely favoured by the presence of the cysteine/cystine redox couple used during our refolding/purification procedure of CRM197-RBD.

To further inspect the refolding of CRM-RBD, we performed DNase activity assays using the refolded purified protein and, as reference controls, DNase I from bovine pancreas and recombinant full-length CRM197. First, we used bovine DNase I provided by Millipore-Sigma as a standardized formulation containing 2000 Kunitz Units [12] when assayed in the presence of calf thymus DNA supplied by the same provider. When assays were performed using 10 or 30 nominal Kunitz Units of bovine DNase I, we observed an activity corresponding to 9.4 and 25.4 Units, respectively (Supplementary Figs. S6A-S6C), indicating that the DNA substrate can be considered as an appropriate standard material. Then, we assayed the DNase activity exerted by 25 μg of recombinant full-length CRM197 (Supplementary Fig. S6D), and we detected 6.1 Kunitz Units (Supplementary Fig. S6E). Finally, when the activity exerted by 15 μg of CRM197-RBD was tested (Supplementary Fig. S6D), we observed a DNase action corresponding to 2.6 Kunitz Units (Supplementary Fig. S6F). This level of activity suggests that CRM197-RBD was properly refolded by the procedures we used during its purification, as it was previously reported for recombinant full-length CRM197 refolded and purified from *E. coli* inclusion bodies treated with chaotropic agents [8–10,19].

When the stability of recombinant full-length CRM197 was inspected by CD spectroscopy a melting temperature (T_m) equal to 58 °C was determined [20], suggesting for this protein an effective stability at room temperature. We therefore decided to test the conformational stability of CRM197-RBD by means of far-UV CD spectroscopy. In particular, a solution of 0.3 or 1 μM CRM-RBD was kept at ambient temperature in a quartz cuvette, and CD spectra were recorded as a function of time. Under these conditions, CRM197-RBD featured a satisfactory stability over 24 h, with consistent denaturation occurring after 48–54 h of residence at room temperature (Supplementary Fig. S7). It is important to note that a couple of stability tests performed with two independent purification batches of CRM197-RBD yielded very similar observations (Supplementary Fig. S7).

The human angiotensin-converting enzyme 2 (ACE2) receptor is known to represent the target of COVID-19 spike protein RBD [21,22]. Quantitatively speaking, K_D values over the 1.2–44.2 nM concentration interval were reported for the association of human ACE2 to the RBD of COVID-19 spike protein [21,22], indicating a tight association between the two protein partners. To test the binding of purified CRM197-RBD chimera to the human receptor we performed surface plasmon resonance (SPR) assays. Remarkably, we observed an efficient binding between the immobilized target and the CRM197-RBD chimera, yielding a K_D value equal to

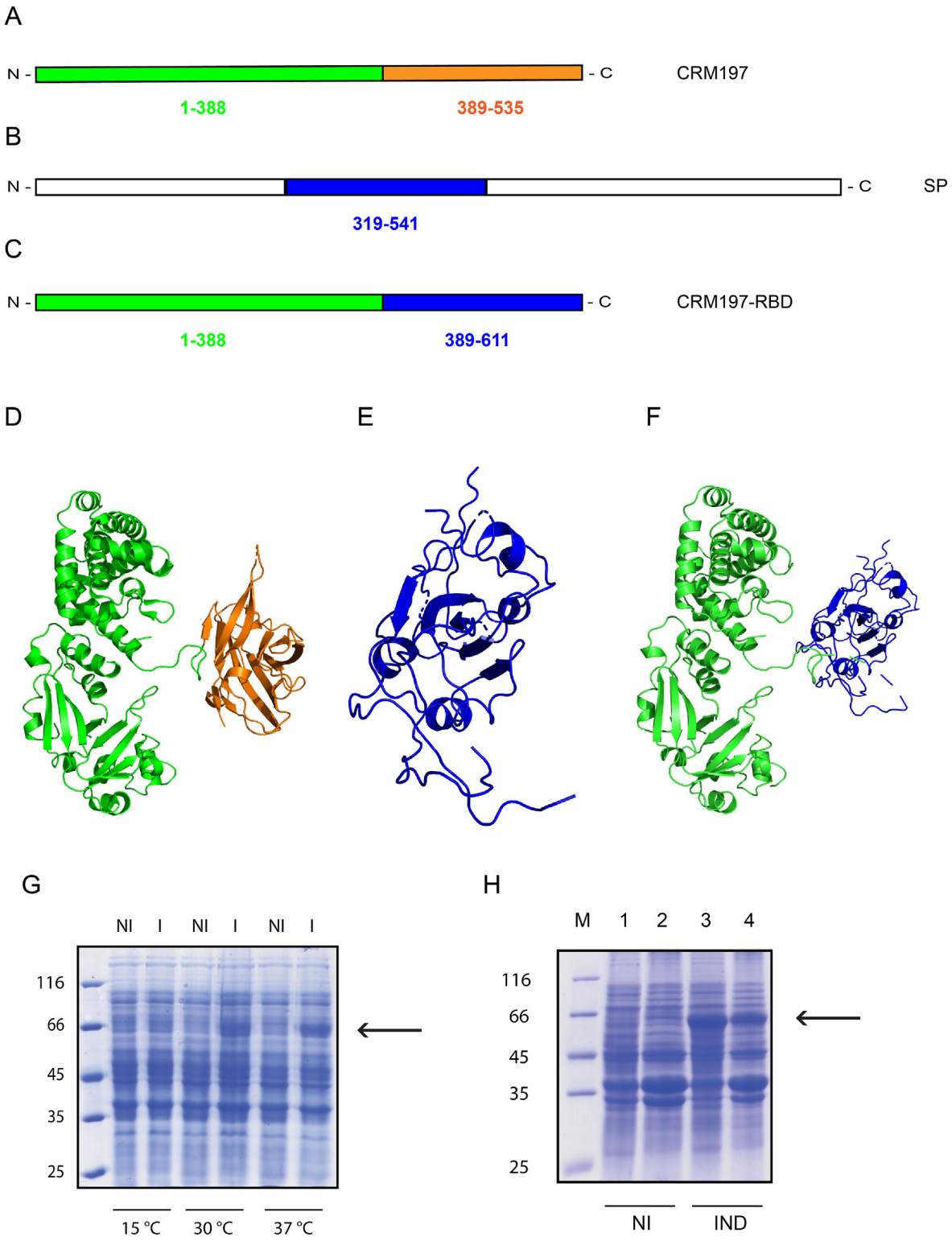

Fig. 1. Construction of the CRM197-RBD chimera and overexpression in *Escherichia coli*. A-C) Cartoons representing the primary structure of CRM197 (**A**), COVID-19 spike protein (**B**), and CRM197-RBD chimera (**C**). The structural regions of CRM197 shown in green and orange (**A**) correspond to the catalytic-transmembrane domains and to the HB-EGF receptor-binding domain, respectively. The portion of spike protein reported in blue (**C**) denotes the receptor-binding domain. **D-F)** Tertiary structure of CRM197 (**D**, PDB file 5i82), of the receptor-binding domain of COVID-19 spike protein (**E**, file PDB 6vyb), and a model (**F**) of the CRM197-RBD chimera. **G)** Electrophoretic analysis of CRM197-RBD expression. Cells of *E. coli* BL21(DE3) transformed with the pET9a-CRM197RBD construct were cultured at 15, 30, or 37 °C and not-induced (NI) or induced (I) with 1 mM IPTG to express CRM197-RBD. Cells were collected by centrifugation, resuspended in H_2O and electrophoretic sample buffer, boiled for 5 min, and the lysed cells were then subjected to SDS-PAGE. **H)** Cellular localization of overexpressed CRM197-RBD. Pellets containing cells not-induced (NI) or induced (IND) to express CRM197-RBD were lysed by sonication, the protein extract was centrifuged at 4,000 g, and the supernatant accordingly obtained was centrifuged at 19,000 g. The two protein pellets were resuspended in H_2O and electrophoretic sample buffer, boiled for 5 min, and analyzed by SDS-PAGE (lanes 1 and 3: pellets sedimented by centrifugation at 4,000 g; lanes 2 and 4: samples obtained by centrifugation at 19,000 g). (For interpretation of the references to colour in this figure legend, the reader is referred to the Web version of this article.)

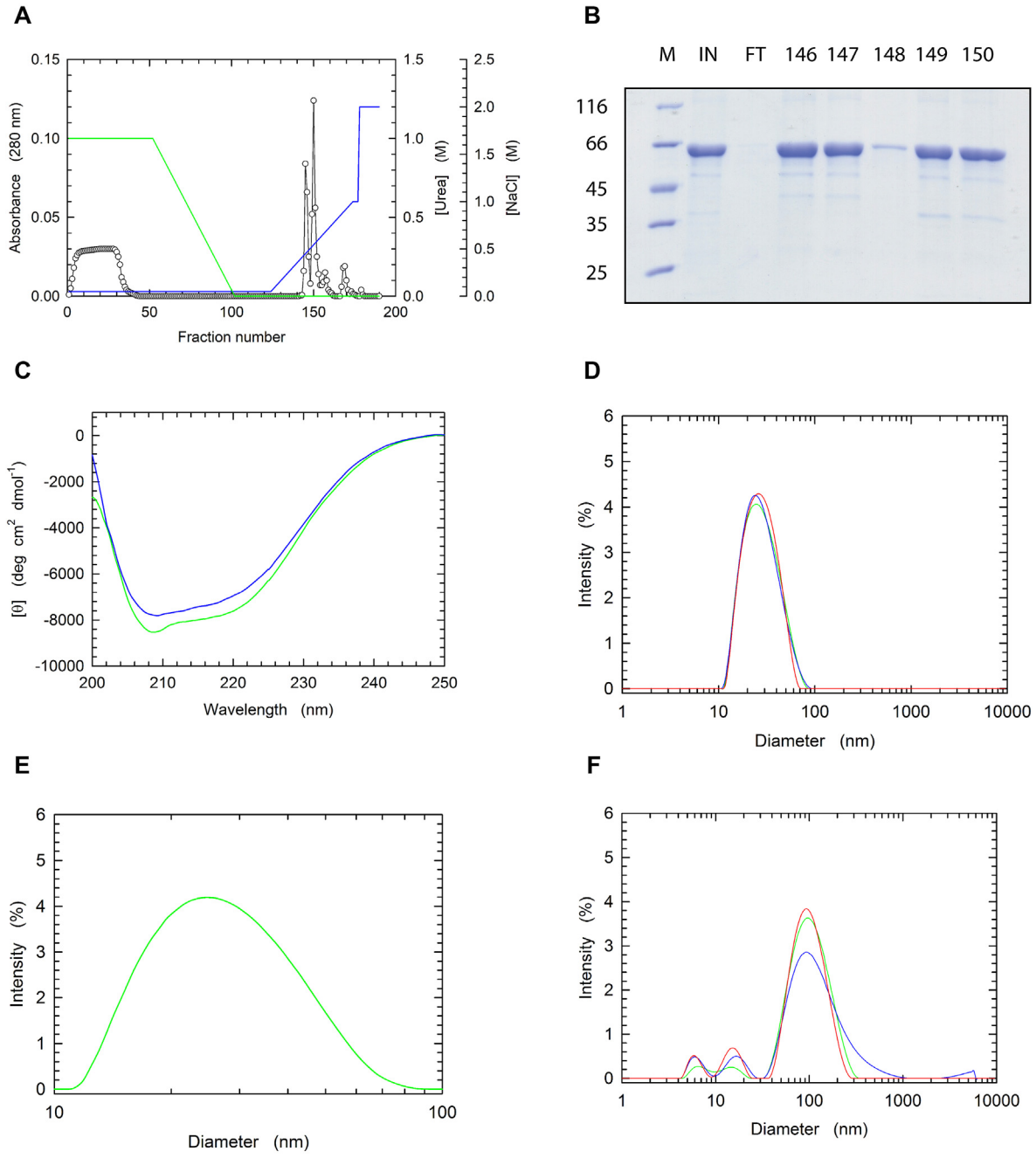

Fig. 2. Purification and characterization of CRM197-RBD. A) Affinity chromatography performed with a HiTrap Heparin column. The urea and NaCl gradients are shown in green and blue, respectively. **B)** SDS-PAGE of representative fractions eluted from the affinity chromatography column. The column input (IN) and flow-through (FT) are also shown. **C** CD spectra of recombinant full-length CRM197 (green line) and of CRM197-RBD (blue line). **D**,**E)** DLS analysis of purified CRM197-RBD. The output of three independent tests is shown (**D**), along with a detail (**E**) of their average. **F)** Characterization by DLS of full-length recombinant CRM197. Three independent observations are shown. (For interpretation of the references to colour in this figure legend, the reader is referred to the Web version of this article.)

10.4 ± 0.9 nM (Supplementary Fig. S8). This observation indicates that the CRM197 portion does not constrain the ACE2-binding proficiency of the RBD grafted to the chimera. Indeed, the presence of a quite extended and flexible linker between the two elements of the chimera (Fig. 1F) may be responsible for conferring to the RBD of spike protein sufficient steric freedom to interact with the receptor.

Finally, to assess the robustness of our strategy for the production of protein chimeras containing the CRM197 platform, we designed a second fusion protein, composed of the residues 1–388 of CRM197 tagged with a short peptide consisting of amino acids 814–826 of COVID-19 SP (Supplementary Fig. S9). This peptide was chosen according to a recent report which suggested this portion of SP as an appropriate target for vaccines [23], when considering its location on the spike protein surface and its high degree of conservation among different coronaviruses [23]. To produce the CRM197-peptide fusion protein (denoted CRM197-PEP) we used the same strategy previously devised for CRM197-RBD, i.e. a synthetic gene optimized for *E. coli* codon usage was synthesized and cloned into pET9a expression vector (Supplementary Fig. S9). Remarkably, high levels of overexpression were detected in *E. coli* BL21(DE3) transformants induced at 37 °C, and the identity of the

A

Observed Molecular mass (Da)	Peptide	Theoretical Molecular mass (Da)
2620.229	11-33	2620.227
1384.554	40-51	1384.553
1002.431	52-59	1002.429
1798.804	60-76	1798.801
877.491	83.90	877.491
888.455	96-103	888.455
2362.201	105-125	2362.198
2666.328	134-157	2666.323
1519.790	158-170	1519.788
3738.662	**(174-190)-(194-210)**	3738.653
791.349	230-236	791.348
2440.199	245-264	2440.191
3635.782	265-299	3635.774

B

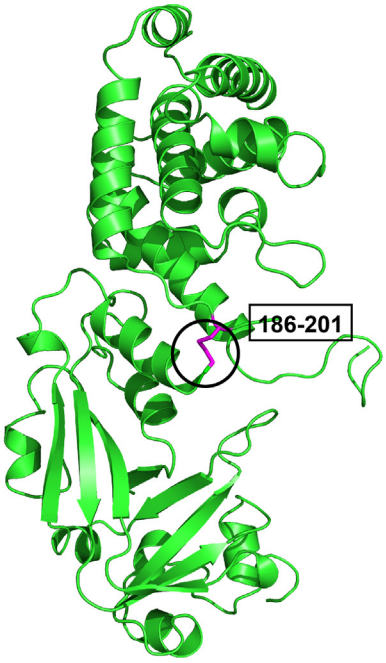

C

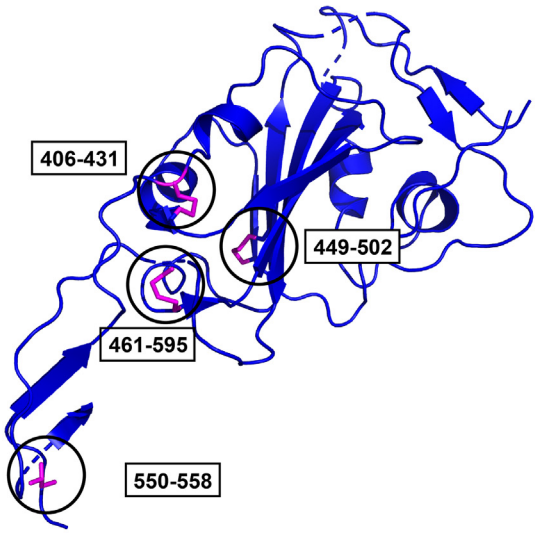

D

Observed Molecular mass (Da)	Peptide	Theoretical Molecular mass (Da)
985.519	390-398	985.519
4352.083	**(399-416)-(428-448)**	4352.055
1112.541	417-425	1112.540
3059.412	**(449-456)-(495-514)**	3059.400
3966.061	**(457-473)-(580-598)**	3966.042
898.491	479-487	898.487
885.423	488-494	885.423
1217.588	515-524	1217.583
989.529	529-536	989.529
4765.115	**537-579 (internal S-S)**	4765.104
660.380	600-605	660.381

Fig. 3. Analysis of the disulphide bridges of the CRM197-RBD chimera by mass spectrometry. A,B) Peptides (**A**) and the C186–C201 disulphide bond (**B**) identified by mass spectrometry in the CRM197 portion of the chimera. **C,D)** The 4 S–S bridges (**C**) detected by mass spectrometry (**D**) within the COVID-19 SP RBD region of the CRM197-RBD chimera.

overexpressed protein was confirmed by mass-spectroscopy (Supplementary Fig. S10). It should be noted that CRM197-PEP does contain only two cysteines, therefore facilitating the refolding from inclusion bodies of the overexpressed protein. In addition, the high level of overexpression of both CRM197-RBD and CRM197-PEP suggests that the fragment containing the residues 1–388 of CRM197 represents a convenient scaffold to which different epitopes can be fused to engineer candidate vaccines.

The strategy we propose here for the production of a fusion vaccine directed against COVID-19 features a number of convenient points. First, the use of *E. coli* as the microbial host for the overexpression of a subunit vaccine implies a fast and robust process when compared with fermentations requiring other microorganisms or higher-organism cells. Further, the isolation from inclusion bodies of a protein vaccine translates into a favourable purification procedure. This is exemplified by the purification procedure reported here for the CRM197-RBD chimera, consisting of a first rapid separation of the protein fraction associated to nucleic acids, a dialysis to lower urea concentration, and a final affinity chromatography step. In addition, contrary to diphtheria and tetanus toxoids, CRM197 was shown to feature modest, if at all, carrier-induced epitopic suppression [24]. It should also be noted that the CRM197-RBD chimera lacks a significant portion of full-length CRM197, i.e. the HB-EGF receptor-binding domain (Supplementary Fig. S11A), but retains major immunogenic determinants of the parent protein. It was indeed shown that B and T cell epitopes reside in fragments A and B, respectively (Supplementary Figs. S11B-S11C) [25,26]. In particular, it was shown that the regions 245–264, 271–290, 299–312, and 321–350 are important T cell epitopes of diphtheria toxin and CRM197 (Supplementary Figs. S11B-S11C) [27–29].

Finally, we showed here that CRM197-RBD does effectively withstand storage at room temperature for 24 h, making this protein chimera a candidate vaccine the use of which would be independent of the cold chain. It is therefore our hope that the strategy presented here for the production of fusion vaccines will expand the repertoire of available approaches.

Funding sources

This research did not receive any specific grant from funding agencies in the public, commercial, or not-for-profit sectors.

Declaration of competing interest

The authors declare that they have no known competing financial interests or personal relationships that could have appeared to influence the work reported in this paper. A.H. dedicates this work to the memory of Dr. Silvio Buzzi.

Appendix A. Supplementary data

Supplementary data to this article can be found online at https://doi.org/10.1016/j.bbrc.2021.04.056.

References

[1] C. Bruce, R.L. Baldwin, S.L. Lessnick, et al., Diphetria toxin and its ADP-ribosyltransferase-defective homologue CRM197 possess deoxyribonuclease activity, Proc. Natl. Acad. Sci. U.S.A. 87 (1990) 2995–2998.
[2] T. Uchida, A.M. Pappenheimer Jr., R. Greany, Diphteria toxin and related proteins. I. Isolation and properties of mutant proteins serologically related to diphteria toxin, J. Biol. Chem. 248 (1973) 3838–3844.
[3] S. Lory, S.F. Carroll, R.J. Collier, Ligand interactions of diphtheria toxin. II. Relationships between the NAD site and the P site, J. Biol. Chem. 255 (1980) 12016–12019.
[4] M. Porro, M. Saletti, L. Nencioni, et al., Immunogenic correlation between Cross-Reacting Material (CRM197) produced by a mutant of *Corynebacterium diphtheriae* and diphtheria toxoid, J. Infect. Dis. 142 (1980) 716–724.
[5] R. Rappuoli, E. De Gregorio, P. Costantino, On the mechanism of conjugate vaccines, Proc. Natl. Acad. Sci. U.S.A. 116 (2019) 14–16.
[6] T.K. Tan, P. Rijal, R. Rahikainen, et al., A COVID-19 vaccine candidate using SpyCatcher multimerization of the SARS-CoV-2 spike protein receptor-binding domain induces potent neutralising antibody responses, Nat. Commun. 12 (2021) 542.
[7] P.M. Moyle, Biotechnology approaches to produce potent, self-adjuvanting antigen-adjuvant fusion protein subunit vaccines, Biotechnol. Adv. 35 (2017) 375–389.
[8] A. Stefan, M. Conti, D. Rubboli, et al., Overexpression and purification of the recombinant diphtheria toxin variant CRM197 in *Escherichia coli*, J. Biotechnol. 156 (2011) 245–252.
[9] A. Stefan, M. Boiani, L. Longanesi, et al., On-column refolding of diphtheria toxin variant CRM197 by different metal-chelating affinity chromatography matrices, J. Chem. Chem. Eng. 8 (2014) 1135–1141.
[10] R.P.N. Mishra, R.S.P. Yadav, C. Jones, et al., Structural and immunological characterization of *E. coli* derived recombinant CRM_{197} protein used as carrier in conjugate vaccines, Biosci. Rep. 38 (2018) 1–14.
[11] M.A. Bradford, A rapid and sensitive method for the quantitation of microgram quantities of protein utilizing the protein-dye binding, Anal. Biochem. 72 (1976) 248–254.
[12] M. Kunitz, Crystalline desoxyribonuclease. I. Isolation and general properties. Spectrophotometric method for the measurement of desoxyribonuclease activity, J. Gen. Physiol. 22 (1950) 349–362.
[13] A. Schevchenko, H. Tomas, J. Havliš, et al., In-gel digestion for mass spectrometric characterization of proteins and proteomes, Nat. Protoc. 1 (2007) 2856–2860.
[14] E. Conte, G. Vincelli, R.M. Schaaper, et al., Stabilization of *the Escherichia coli* DNA polymerase III ε subunit by the θ subunit favors *in vivo* assembly of the Pol III catalytic core, Arch. Biochem. Biophys. 523 (2012) 135–143.
[15] M. Wojdyr, Fityk: a general-purpose peak fitting program, J. Appl. Crystallogr. 43 (2010) 1126–1128.
[16] A.-W. Struck, M. Axmann, S. Pfefferle, et al., A hexapeptide of the receptor-binding domain of SARS corona virus spike protein blocks viral entry into host cells via the human receptor ACE2, Antivir. Res. 94 (2012) 288–296.
[17] E. Malito, B. Bursulaya, C. Chen, et al., Structural basis for lack of toxicity of the diphtheria toxin mutant CRM197, Proc. Natl. Acad. Sci. U.S.A. 109 (2012) 5229–5234.
[18] B. Steere, D. Eisenberg, Characterization of high-order diphtheria toxin oligomers, Biochemistry 39 (2000) 15901–15909.
[19] N. Bravo-Bautista, H. Hoang, A. Joshi, et al., Investigating the deoxyribonuclease activity of CRM197 with site-directed mutagenesis, ACS Omega 4 (2019) 11987–11992.
[20] J.M. Hickey, V.M. Toprani, K. Kaur, et al., Analytical comparability assessments of 5 recombinant CRM_{197} proteins from different manufacturers and expression systems, J. Pharmacol. Sci. 107 (2018) 1806–1819.
[21] J. Shang, G. Ye, K. Shi, et al., Structural basis of receptor recognition by SARS-CoV-2, Nature 581 (2020) 221–224.
[22] A.C. Walls, Y. Park, M.A. Tortorici, et al., Structure, function, and antigenicity of the SARS-CoV-2 spike glycoprotein, Cell 180 (2020) 281–292.
[23] B. Robson, COVID-19 coronavirus spike protein analysis for synthetic vaccines, a peptidomimetic antagonist, and therapeutic drugs, and analysis of a proposed achilles' heel conserved region to minimize probability of escape mutations and drug resistance, Comput. Biol. Med. 121 (2020) 1–28.
[24] M. Tontini, F. Berti, M.R. Romano, et al., Comparison of CRM_{197}, diphtheria toxoid and tetanus toxoid as protein carriers for meningococcal glycoconjugate vaccines, Vaccine 31 (2013) 4827–4833.
[25] A.M. Pappenheimer Jr., T. Uchida, A.A. Harper, An immunological study of the diphteria toxin molecule, Immunohistochemistry 9 (1972) 891–906.
[26] F. Tribel, B. Autran, S. De Roquefeuil, et al., Immune response to diphteria toxin and to different CNBr fragments: evidence for different B and T cell reactivities, Eur. J. Immunol. 16 (1986) 47–53.
[27] B.M. Diethelm-Okita, D.K. Okita, L. Banaszak, et al., Universal epitopes from human $CD4^+$ cells on tetanus and diphteria toxins, J. Infetc. Dis. 181 (2000) 1001–1009.
[28] E.G. Leonard, D.H. Canaday, C.V. Harding, et al., Antigen processing of the heptavalent pneumococcal conjugate vaccine carrier protein CRM_{197} differs depending on the serotype of the attached polysaccharide, Infect. Immun. 71 (2003) 4186–4189.
[29] P. Wantuch, L. Sun, R.K. LoPilato, et al., Isolation and characterization of new human carrier peptides from two important vaccine immunogens, Vaccine 38 (2020) 2315–2325.